Supplementary Information

Multi-resonant thermally-activated delayed fluorescence (MR-TADF) emitters for blue organic light-emitting transistors (OLETs)

Georgios Fanourakis[1,], Amirhossein Azari[1], and Caterina Soldano[1,2,*]*

[1]Department of Electronics and Nanoengineering, School of Electrical Engineering,

Aalto University, 02150 Espoo, Finland

[2]Quantum Materials and Sensing Institute, Northeastern University, Burlington, MA, 01803 USA

* Corresponding authors

GF: georgios.fanourakis@aalto.fi

CS: caterina.soldano@aalto.fi

(a) Thermally-Activated Delayed Fluorescence (TADF) and Multi-Resonant TADF Mechanisms

Figure S1a depicts the energy levels of the ground state (S_0) and the first excited state (S_1) (the T_1 responsible for intersystem crossing (ISC) and reverse intersystem crossing (RISC) is not shown in the picture). Upon excitation, an electron occupies the first excited singlet state S_1 and the relaxation to the ground state occurs through radiative emission of a photon from the lowest vibrational level of the excited state. In conventional TADF materials, the ground state has different vibrational sublevels, all of which are accessible to the excited electron. Therefore, recombination from the S_1 to different vibrational levels of S_0 occurs and leads to a broadened emission spectrum. Multi-resonant thermally-activated delayed fluorescence (MR-TADF) materials achieve HOMO-LUMO separation due to the electron rich (N) and electron deficient (B) atoms that are arranged in a para-position, leading to a small difference (<0.2 eV) between first triplet state T_1 and the first singlet S_1. Their rigid structure exhibits fewer vibrational levels and reduced vibronic coupling (smaller Stokes swifts, **Figure S1b**), thus resulting in a narrower

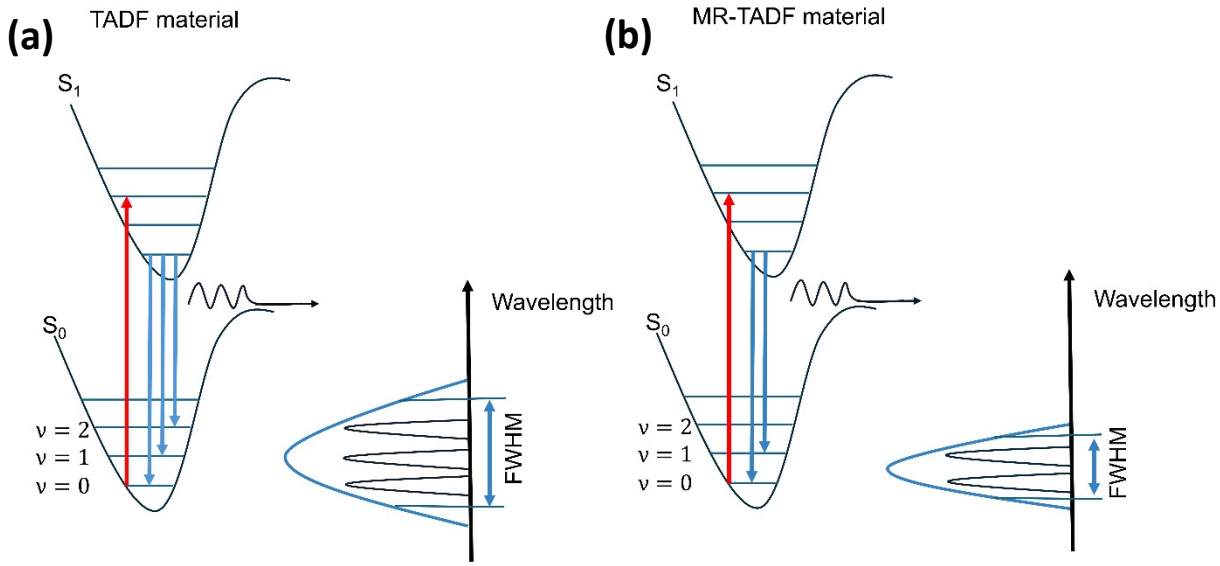

Figure S1. Jablonski diagram of (a) a conventional TADF and (b) a multi-resonant TADF materials, with corresponding emission.

emission spectrum compared to conventional TADF materials.

(b) Optical characterization of MR-TADF-based blends

Figure S2 shows the absolute photoluminescence spectra at room temperature, excited with a 325 nm He-Cd laser system for different DPEPO:*t*-DABNA blend concentrations deposited on Si/SiO_2. These are the same data as presented in **Figure 1a** in the main manuscript. We observed an increase in the photoluminescence from 5% guest concentration to 10%, while for higher concentrations the photoluminescence intensity decreases; PL is further quenched for *t*-DABNA neat film (dashed line). All blends exhibited broadening of the spectrum at higher wavelengths for increasing concentration, where we attribute the main additional component to excimer formation at high emitter content. For *t*-DABNA neat film the excitonic peak is almost completely quenched and most of the emission arises at lower energies.

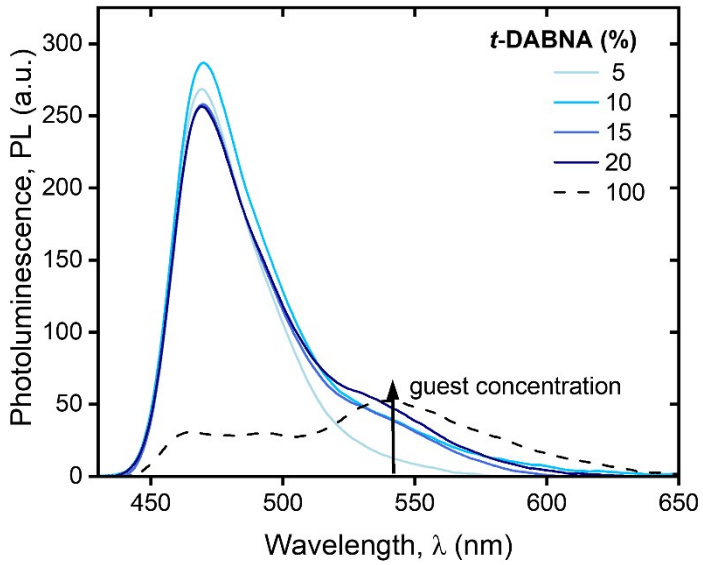

Figure S2. Room temperature photoluminescence of DPEPO:*t*-DABNA blends on Si/SiO_2 substrate with different *t*-DABNA concentration (as labelled). Dashed line represents the PL of a neat *t*-DABNA film.

Table T1 summarizes the main characteristics of the photoluminescence (main emission peak and FWHM) for DPEPO:*t*-DABNA emissive blends on Si/SiO_2 as function of the *t*-DABNA concentration. We do not observe any variation of the peak position for the different *t*-DABNA concentrations.

Table T1. Main peak position and FWHM for photoluminescence spectra for our DPEPO:*t*-DABNA blends deposited on Si/SiO_2 for different *t*-DABNA content.

t-DABNA concentration (%)	Main emission peak wavelength (nm)	FWHM (nm)
5	469	38
10	470	40
15	470	40
20	469	42
100	465	-

(c) Optoelectronic characterization of MR-TADF-based OLET

Figure S3a shows the external quantum efficiency (EQE) as a function of the applied gate voltage; EQE remains approximately constant within the operating regime (saturation). Organic light-emitting transistors with *t*-DABNA concentration of 10% exhibit a value of EQE which is almost two-times higher than the other concentrations. **Figure S3b** shows the color coordinates of our OLETs at different concentrations on a CIE 1931 map (see also **Table T2**). A change in emission colour is observed with increasing *t*-DABNA content.

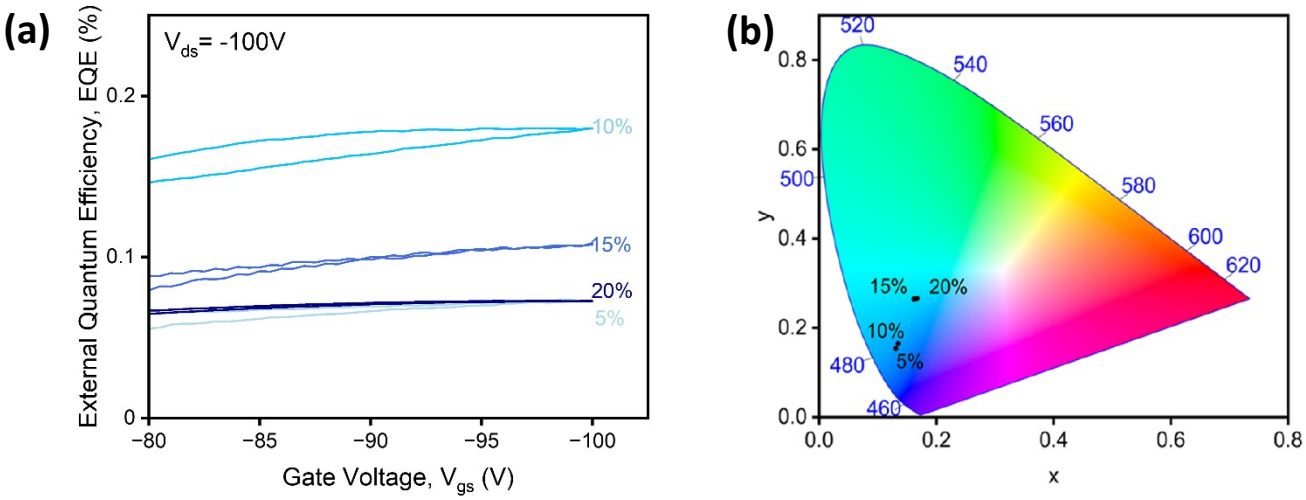

Figure S3. (a) External quantum efficiency as a function of gate voltage V_{gs} (at V_{ds} = -100 V) of our OLETs with different DPEPO:*t*-DABNA blends (as labelled). (b) CIE 1931 diagram of our electroluminescent OLETs devices with different DPEPO:*t*-DABNA blends.

Table T2. Color coordinates for OLETs with different t-DABNA content.

t-DABNA content (%)	Colour Coordinates
5	(0.13, 0.15)
10	(0.13, 0.16)
15	(0.16, 0.26)
20	(0.17, 0.26)

(d) Surface morphology of *p*-type layer

Figure S4 shows the surface morphology of the C8-BTBT film as deposited on the PMMA layer, as studied by atomic force microscopy. C8-BTBT exhibits an *island*-like growth with an average root-mean square roughness (rms) of approximately 2 nm.

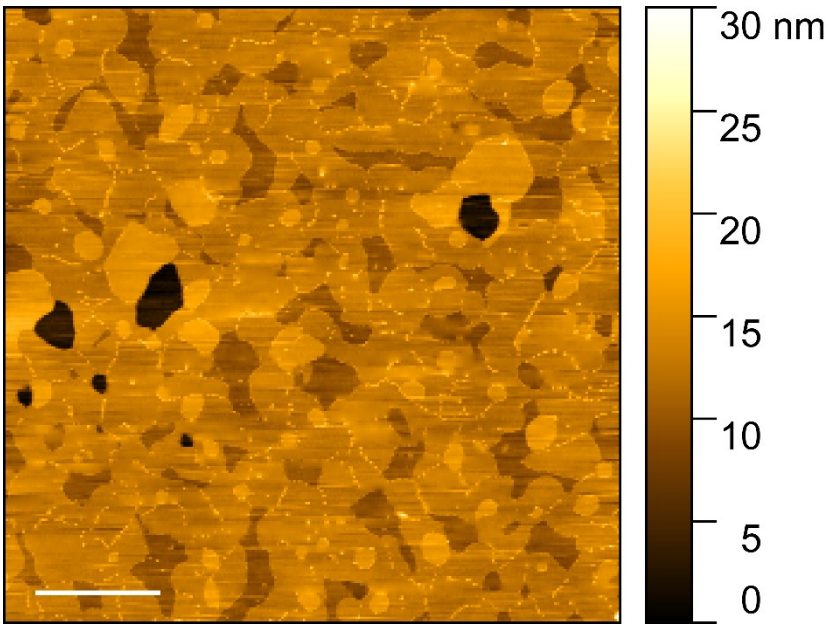

Figure S4. Atomic force microscopy (AFM) micrograph of surface of C8-BTBT (30 nm) as deposited on PMMA dielectric surface. The scan size is 10 µm x 10 µm and scale bar is 2 µm.